Ground-based FTIR Retrievals of PAN at the Polar Environment Atmospheric Research Laboratory

NDACC-IRWG Meeting 2021

June 4, 2021

Tyler Wizenberg, K. Strong,

E. Mahieu & B. Franco

Contact: wizenberg@atmosp.physics.utoronto.ca

Arctic haze observed over the Brooks Range, Alaska during the IPY campaign of 2007-2008.
Image credit J. Cozic NOAA/CIRES.

Outline

- Introduction & Motivation
- The PEARL Bruker IFS 125HR
- SFIT4 Retrievals of PAN
- Results:
  - Retrieved PAN Time Series
  - Comparisons to GEOS-Chem
  - August 2017 Trace Gas Enhancements
- Conclusions

Introduction - Pollution in the Arctic

- The Arctic frequently experiences poor AQ due to both mid-latitude and scattered local sources [Law *et al.*, 2014; Schmale *et al*., 2018]
- Reductions in Arctic summer sea ice have accelerated the rate of industrialization [Roiger *et al*., 2015]
- Wildfires are also a significant periodic source of Arctic pollution [Roiger et al., 2011; Viatte et al., 2013, 2014; Lutsch et al., 2016, 2019]
- Transport pathways and effects on the Arctic environment are not fully understood [Arnold *et al.*, 2016]

An oil drilling rig in the NWT. Photo credit: Getty Images

Introduction - Arctic Haze

- Even the earliest Arctic explorers noted a thin haze in the air, and dirty snow deposits [Nordenskiöld, 1883]
- The ‘Arctic haze’ pollution phenomenon has a pronounced seasonal cycle
- Primarily composed of sulfate aerosols, organic particulate matter, black carbon, tropospheric O_3 and O_3 precursors (NO_X, PAN & VOC’s) [Law et al., 2007, 2014]
- The haze has a measurable positive radiative forcing effect [Ritter *et al*., 2005]

Image credit J. Cozic NOAA/CIRES.

Introduction - PAN in the Arctic

- Lifetime of PAN is strongly temperature dependent
  - Ranges from 1 hour @ 298 K, to several weeks in the cold layers of the UTLS
- Can be transported vast distances to the Arctic where it can influence NO_x and O_3 budgets [Glatthor *et al*., 2007; Tereszkchuk *et al*., 2013]
- Found to be the dominant form of odd nitrogen (NO_y) in the Arctic [Liang *et al*., 2011]

Peroxyacetyl Nitrate ($CH_3C(O)OONO_2$, PAN)

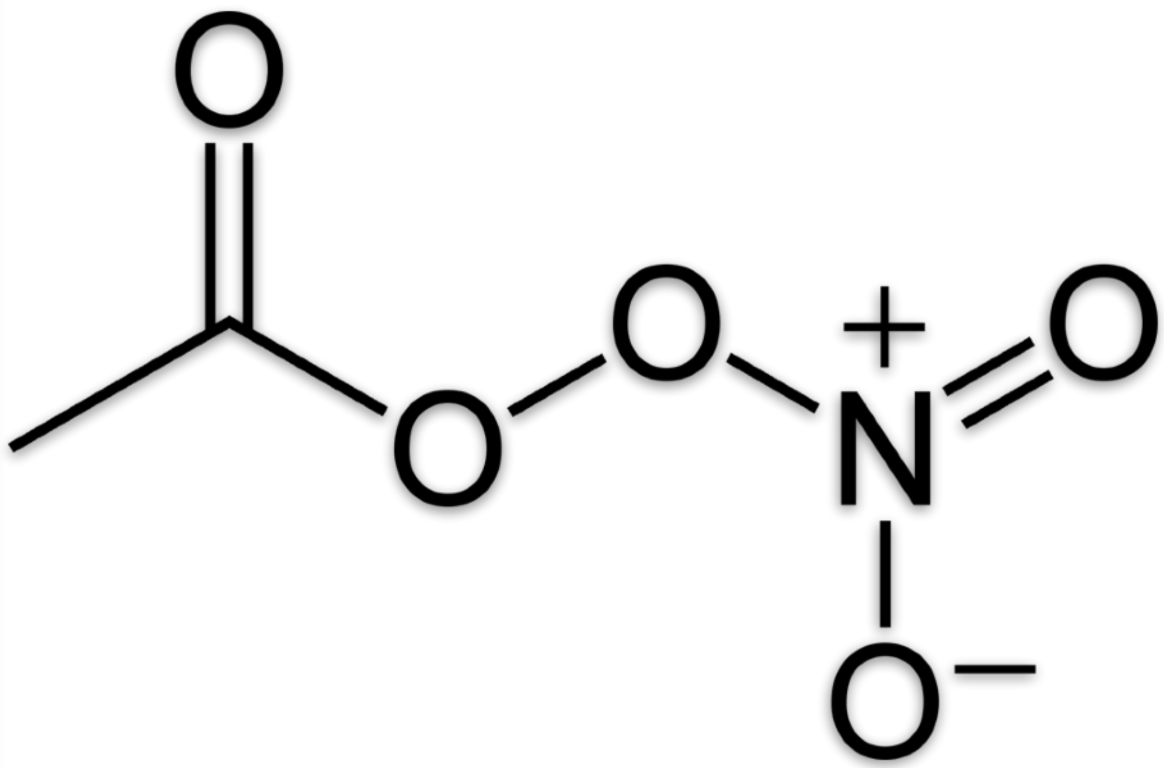

Image source: Wikimedia

Motivation

- Previous measurements have been on a short-term campaign basis [Singh *et al*., 1992; Alvarado *et al*., 2010; Liang *et al*., 2011]
- Recently, satellites have begun to measure PAN (e.g., ACE-FTS, TES and IASI) [Tereszchuk *et al*., 2013; Fischer et al., 2018; Franco *et al*., 2018]
  - Lack of ground-based high latitude measurements for validation
- Influence of wildfires on the PAN budget in the high Arctic has not been well characterized

View from the zeppelin station near Ny-Ålesund, Svalbard (top) during clear conditions, and (bottom) when agricultural fire plumes from Eastern Europe were transported to the station. Photo credit: A.-C. Engvall, Stockholm University.

Motivation

Goals of this work:

1) Develop and apply a new retrieval scheme for PAN to PEARL solar absorption spectra

2) Construct a time series of PAN total columns at Eureka

3) Identify enhancements in PAN which can be linked to biomass burning events

Photo credit: National Park Service / Mike Lewelling

The PEARL Bruker IFS 125HR

- Located at the Polar Environment Atmospheric Research Laboratory (PEARL) in Eureka, NU (80.05°N, 86.42°W, 610m ASL)
    - In operation July 2006 - present
- Custom built Community Solar Tracker (CST) follows the sun and directs the solar beam to the instrument
- Measurements made during clear conditions from polar sunrise in late February to mid-October each year

Photo credit: Me (top), Erik Lutsch (bottom)

SFIT4 Retrieval of PAN

- Retrievals performed using SFIT4 v0.9.4.4
- HITRAN 2008 line-list database [Rothman *et al*., 2009]
- *A priori* profile of PAN from Whole Atmosphere Community Climate Model (WACCM) v4.0 [Marsh *et al*., 2013]
- *A priori* covariance matrix constructed using 1st order Tikhonov regularization

See **Mahieu *et al.* (2021)** for detailed description of retrievals

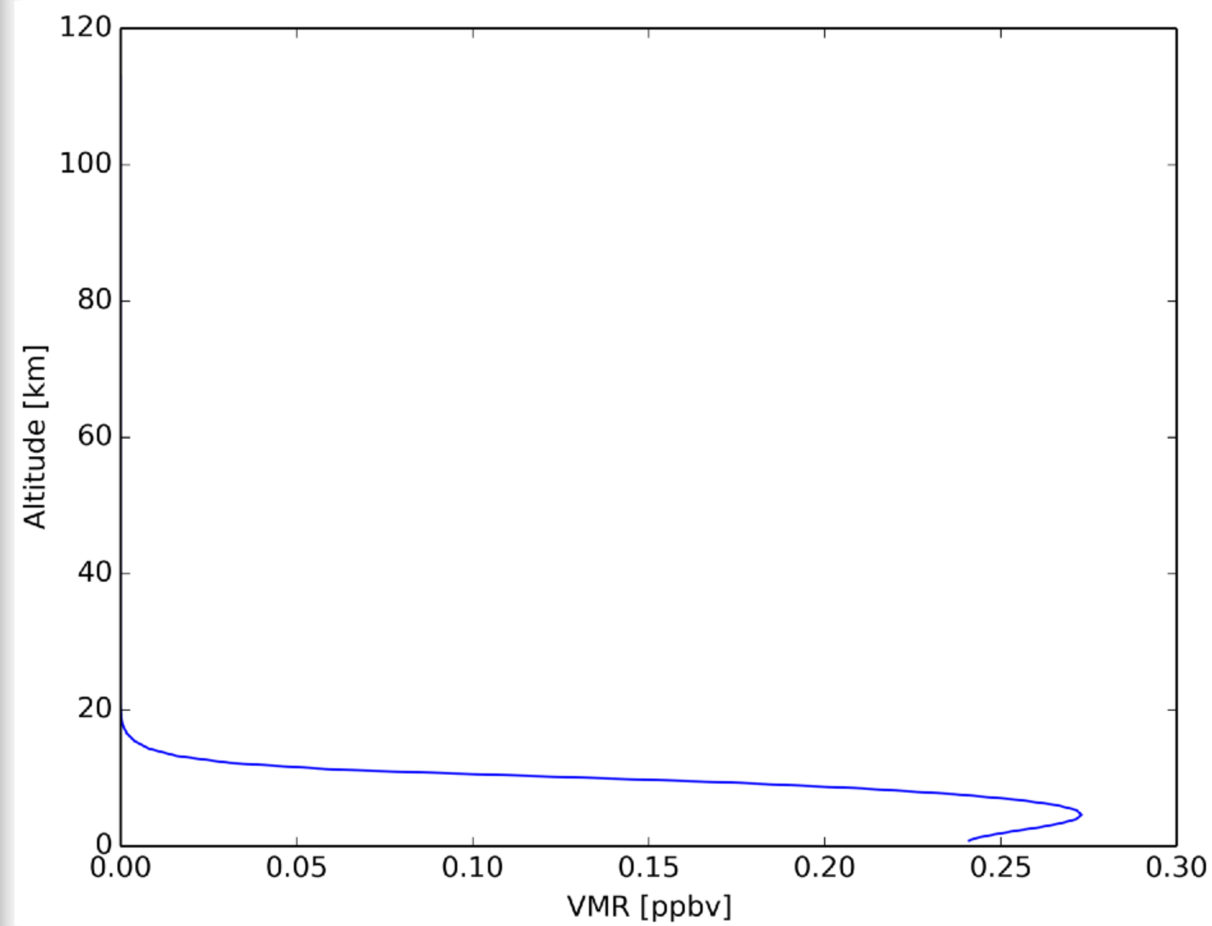

A priori PAN profile from 40-year average of WACCM v4.0

Retrieval Microwindows

Absorption cross-sections of PAN measured @ 295 K. Figure adapted from Allen *et al.*, [2005].

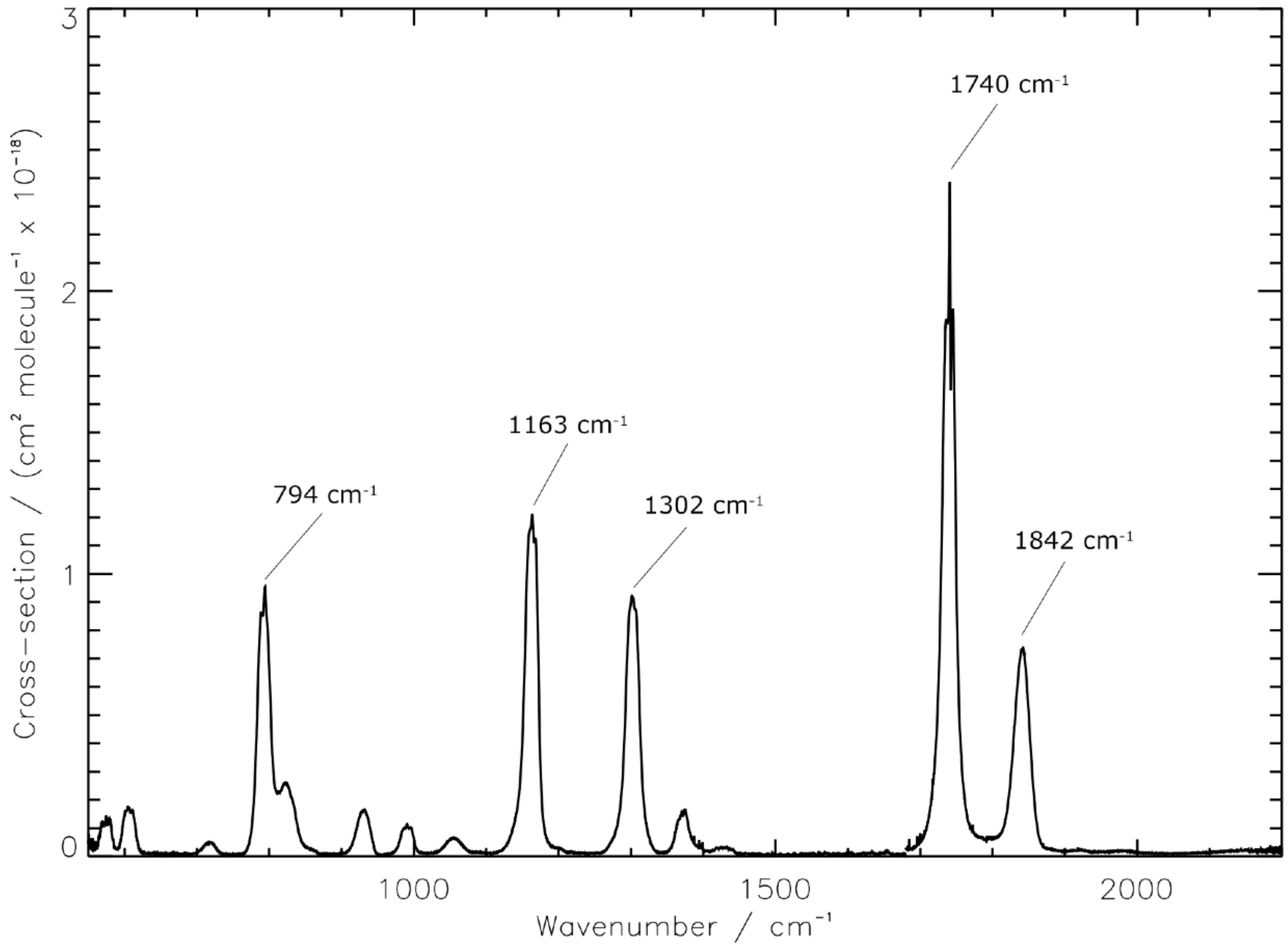

Microwindow #	Wavenumber range (cm^{-1})	Interfering species
1	779.90 - 811.37	H_2O, O_3, CO_2, CCl_4, CHF_2Cl (CFC-22), $ClONO_2$, CFC-113
2	1139.25 - 1179.55	H_2O, HDO, O_3, N_2O, CCl_2F_2, CH_4

Retrieval Microwindows

- Interfering species are also fitted in SFIT4 during the retrieval process

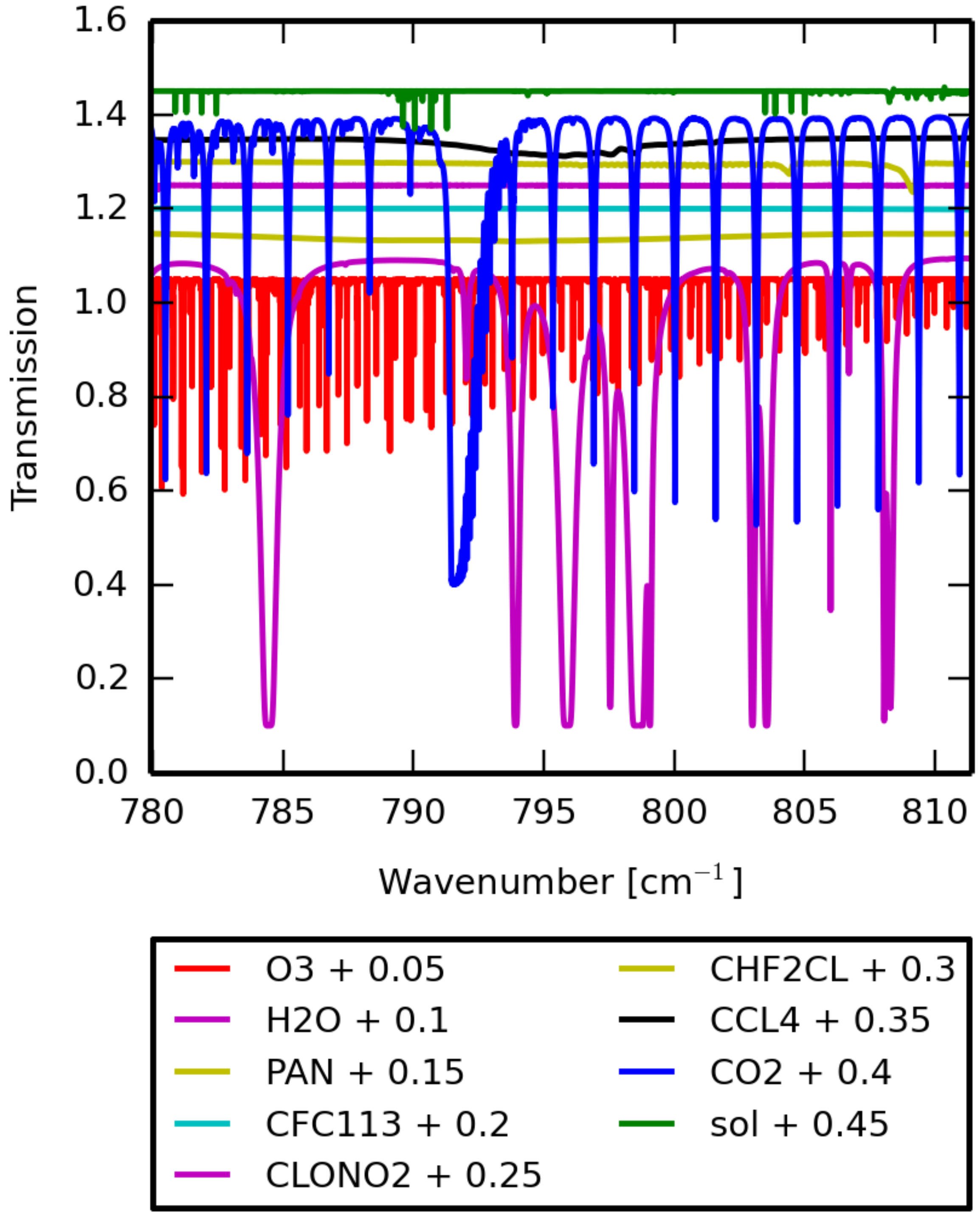

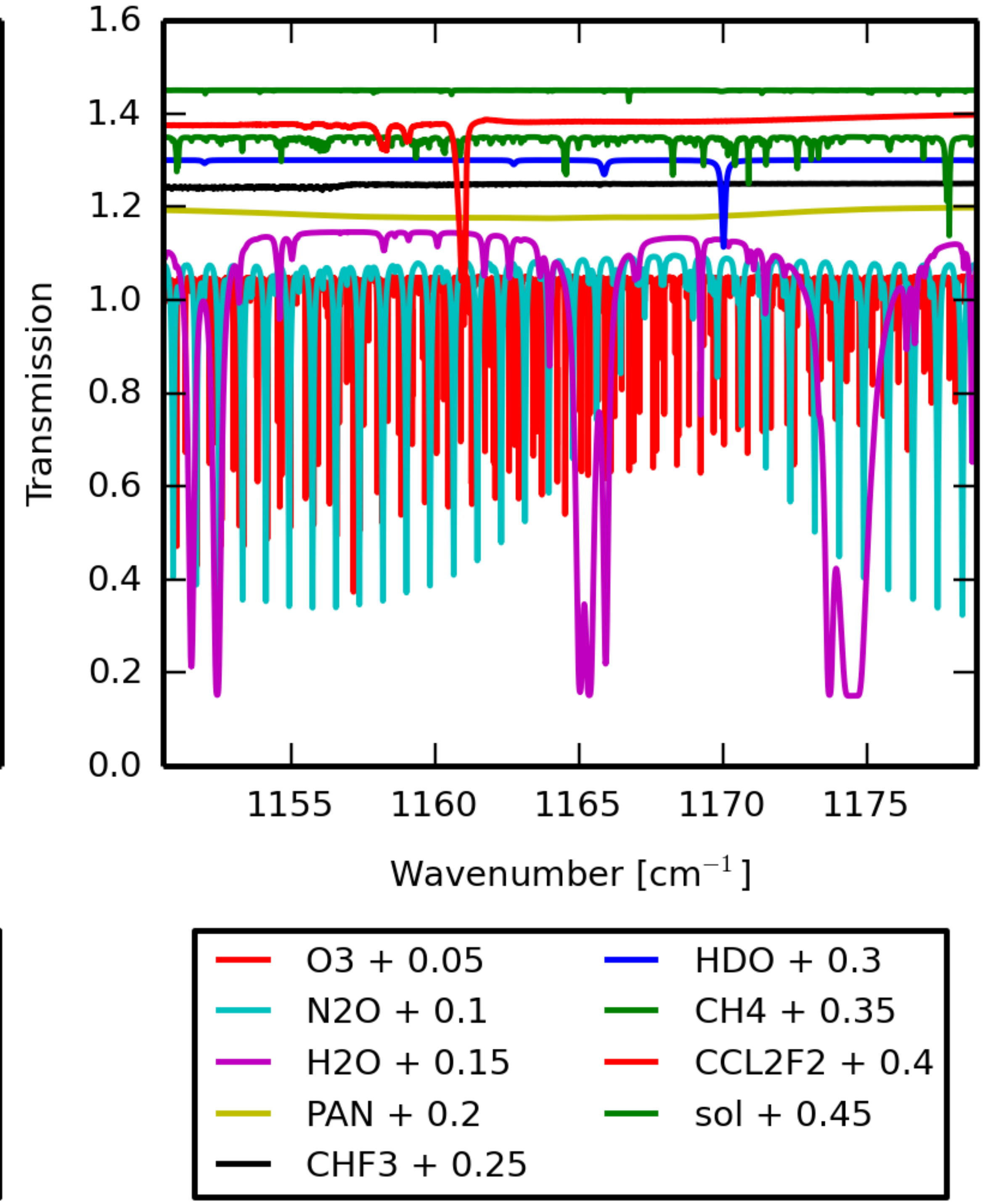

The PAN retrieval microwindows with interfering species included for a spectrum taken at Eureka on Aug. 19, 2017

Averaging Kernels

- **The VMR averaging kernel provides information on the relative contribution of the *a priori* and the measurement to the final retrieved value**

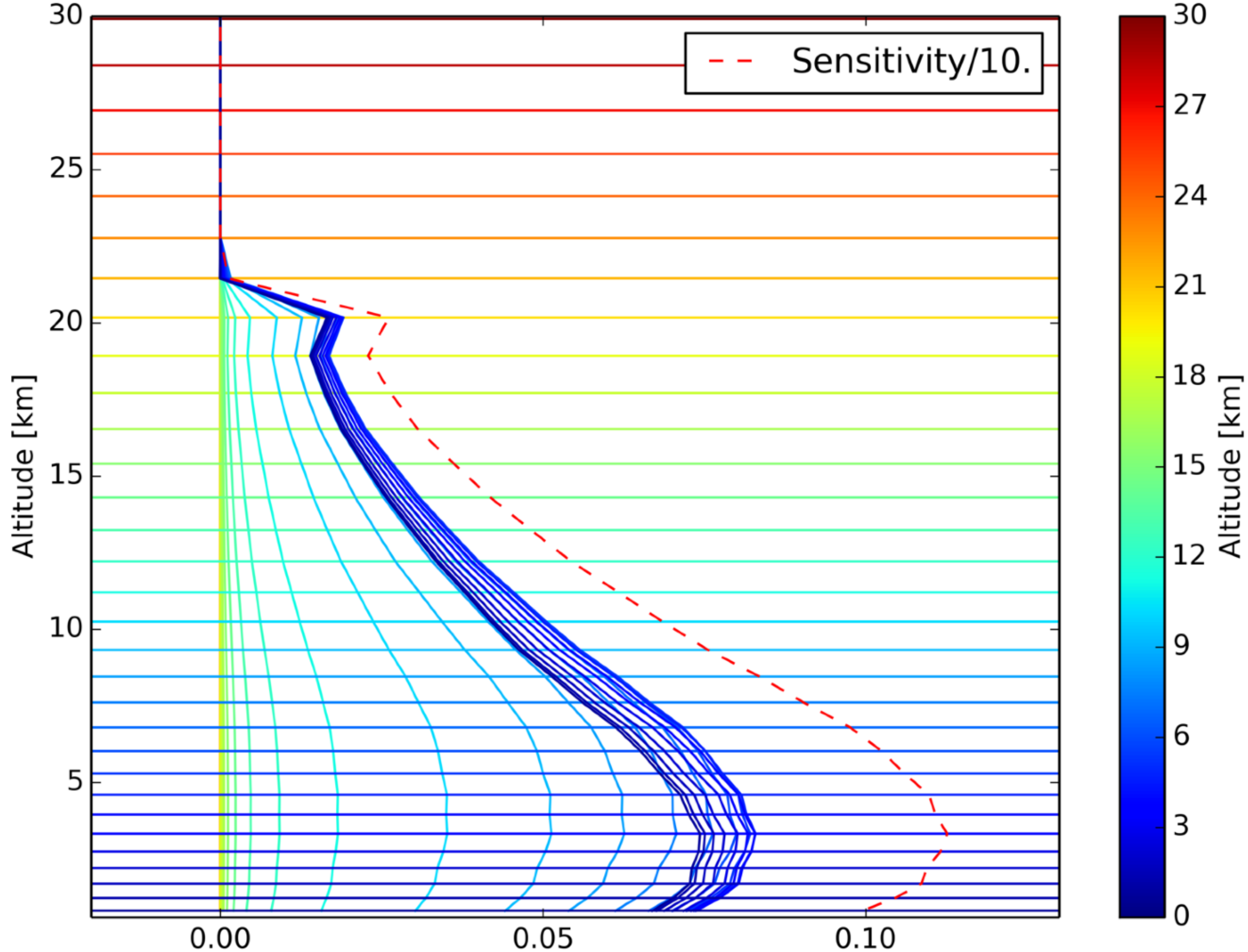

Mean VMR averaging kernel for PAN for 2010-2020.
The sensitivity of the retrieval (scaled by 1/10) is given by the dashed line.

Results - PAN Time Series

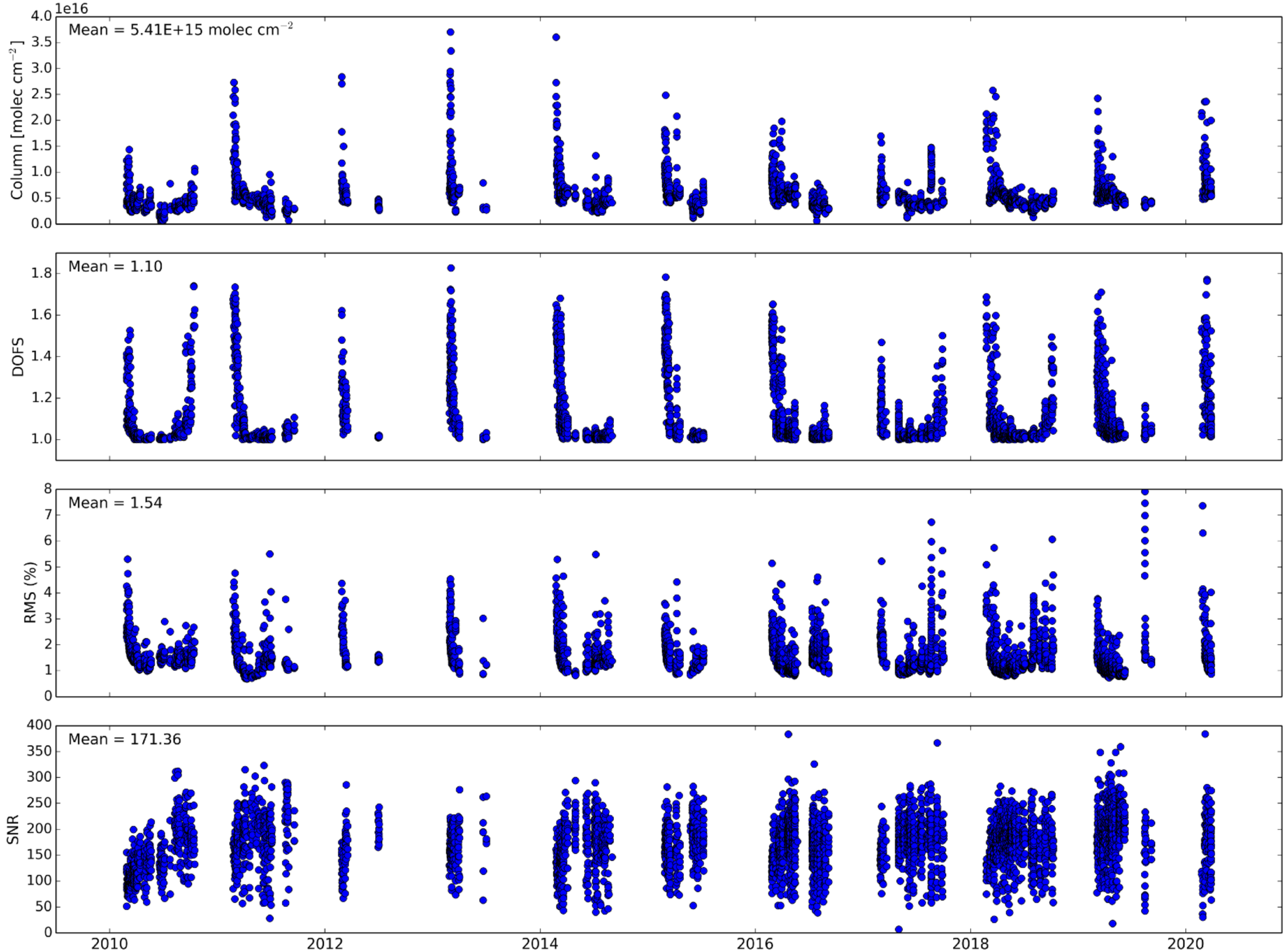

Time series of PAN at Eureka for 2010-2020. The total column concentrations, DOFs, RMS residuals, and the calculated SNR are plotted. Mean values for each are shown in the upper left corner. Note: no filtering was applied yet here.

Results - PAN Time Series

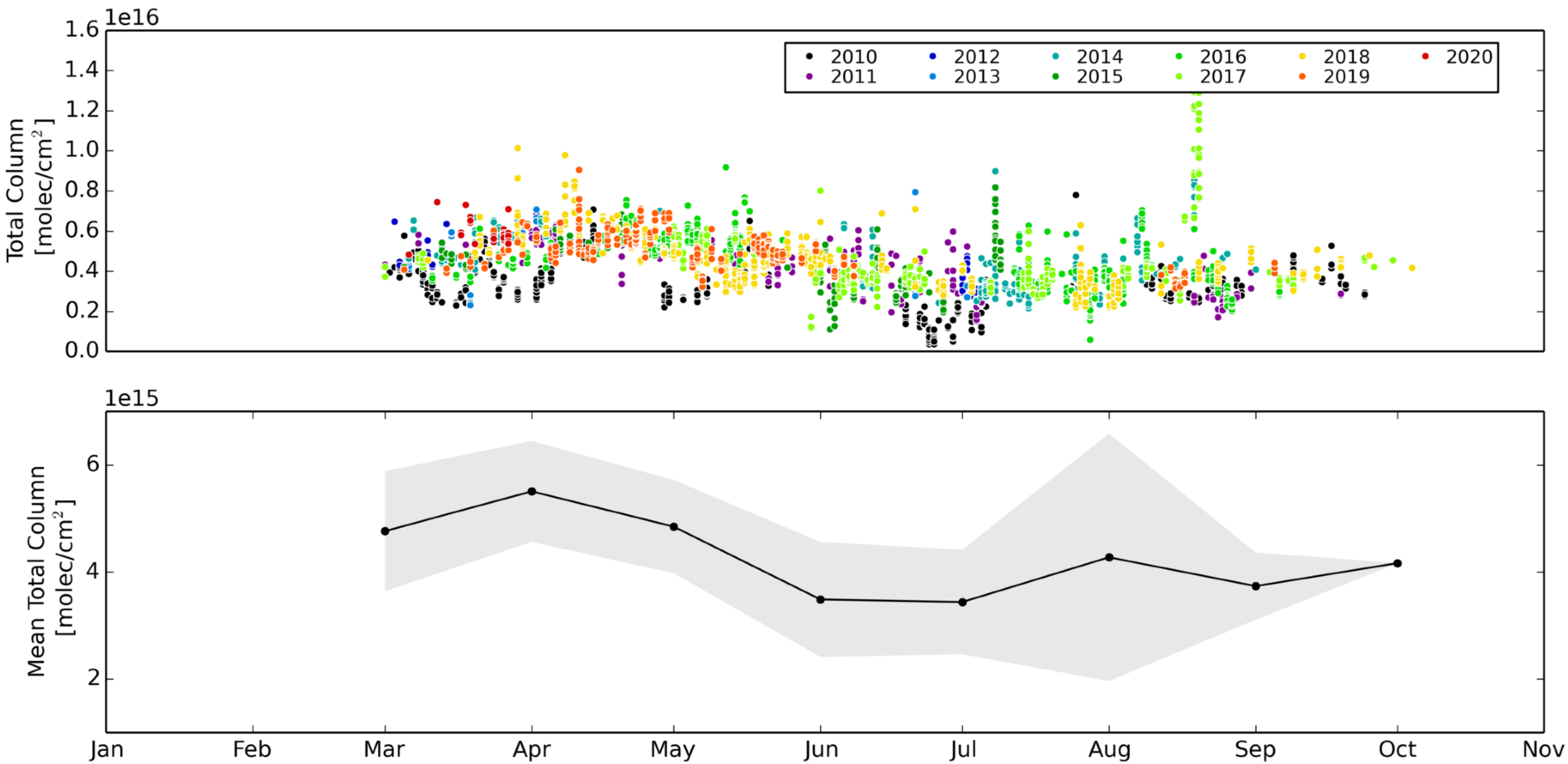

The same time series of PAN total columns at Eureka for 2010-2020 as the previous slide, but all years plotted by month in the top panel, while monthly means are shown in the bottom panel to highlight the seasonal cycle.

Results - GEOS-Chem Comparisons

- GEOS-Chem is a global 3-D atmospheric CTM driven by assimilated met-fields from the Goddard Earth Observing System (GEOS) [Bey *et al*., 2001]

- The simulation of PAN in the model is detailed in Fischer *et al.*, [2014]

- For the comparisons in this work we use GEOS-Chem v12.0.2, with full chemistry included

- This particular simulation was performed by Emmanuel Mahieu of ULiege, Belgium, and covers January 2010 to December 2012

Results - GEOS-Chem Comparisons

Model inputs:

- Meteorological fields from MERRA, v2.0 [Gelaro *et al.*, 2017]
- Fossil fuel emissions: EDGAR [Oliver & Berdowski, 2001] + regional inventories, NMVOC emissions: RETRO [Schultz *et al*., 2007], biogenic emissions: MEGAN [Guenther et al., 2006], and fire emissions: GFED3 [van der Werf et al., 2010]

Model outputs:

- Vertical VMR profiles of PAN at 2-hour intervals on 2°×2.5° (lat/lon) grid centred on PEARL
- Also produces vertical air density profiles, used to convert VMR to partial columns

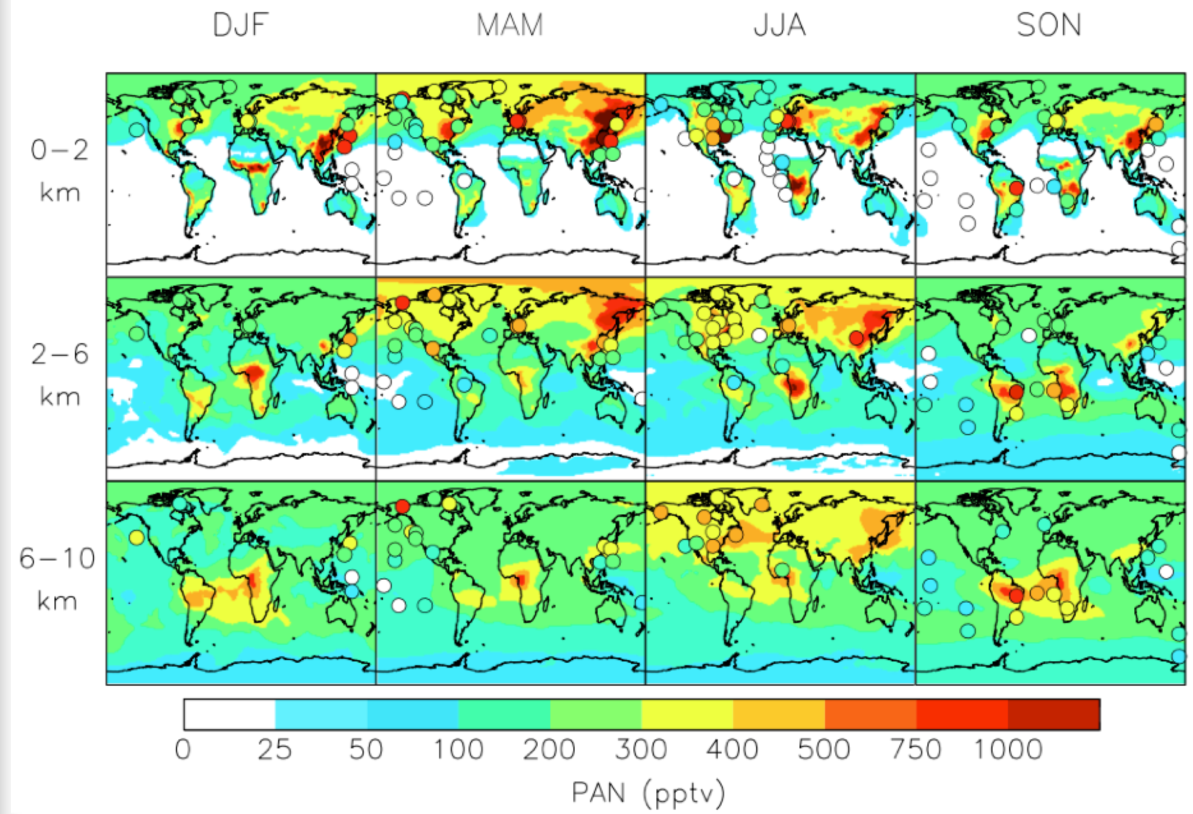

Global mean distribution of PAN from GEOS-Chem for different seasons and altitude ranges. Model results for 2008 are represented by the contours, while the filled circles denote observations from all years. Figure reproduced from Fischer et al., [2014].

Results - GEOS-Chem Comparisons

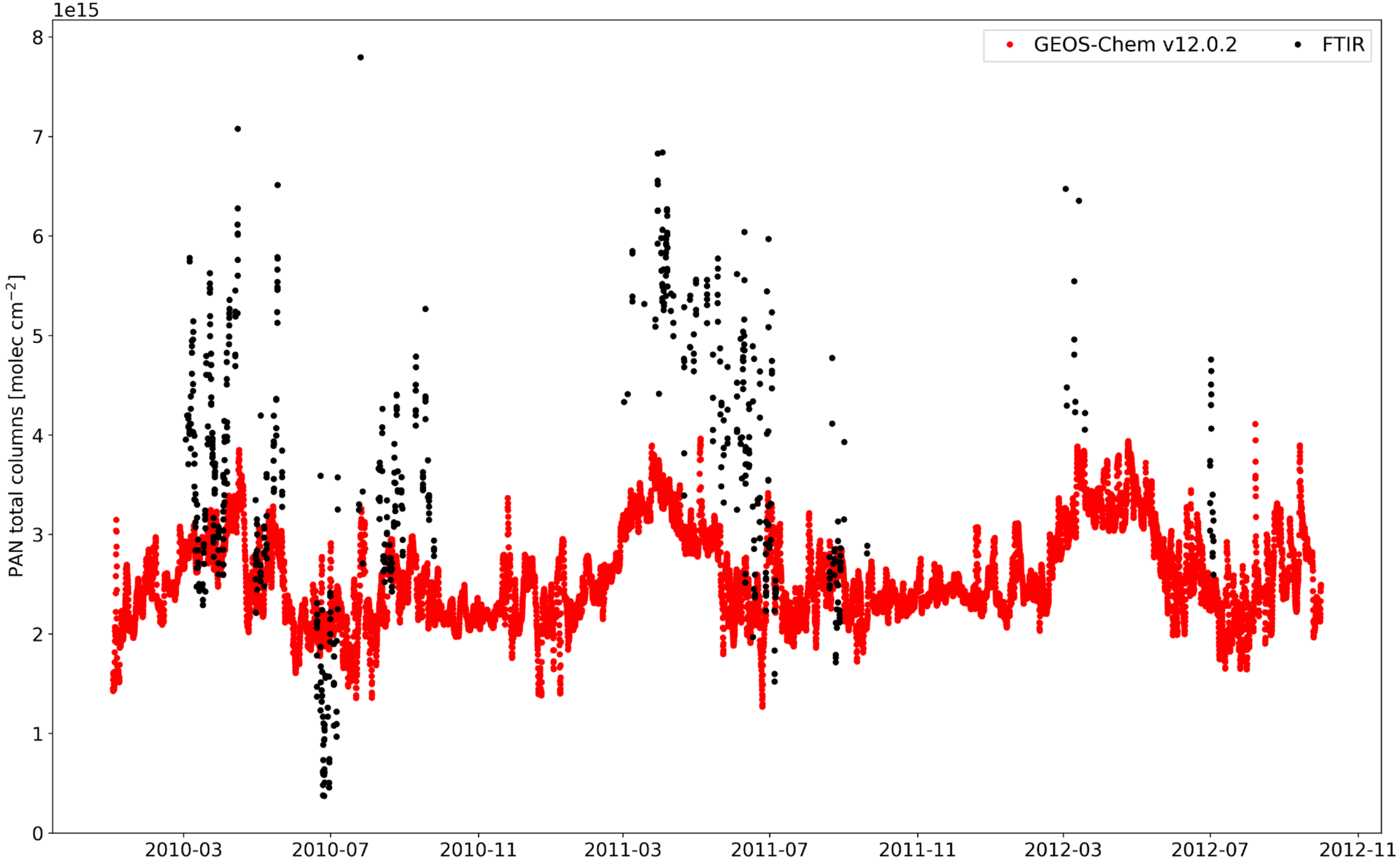

Retrieved PAN total columns overlaid with simulated total columns from GEOS-Chem v12.0.2 at Eureka.

Results - GEOS-Chem Comparisons

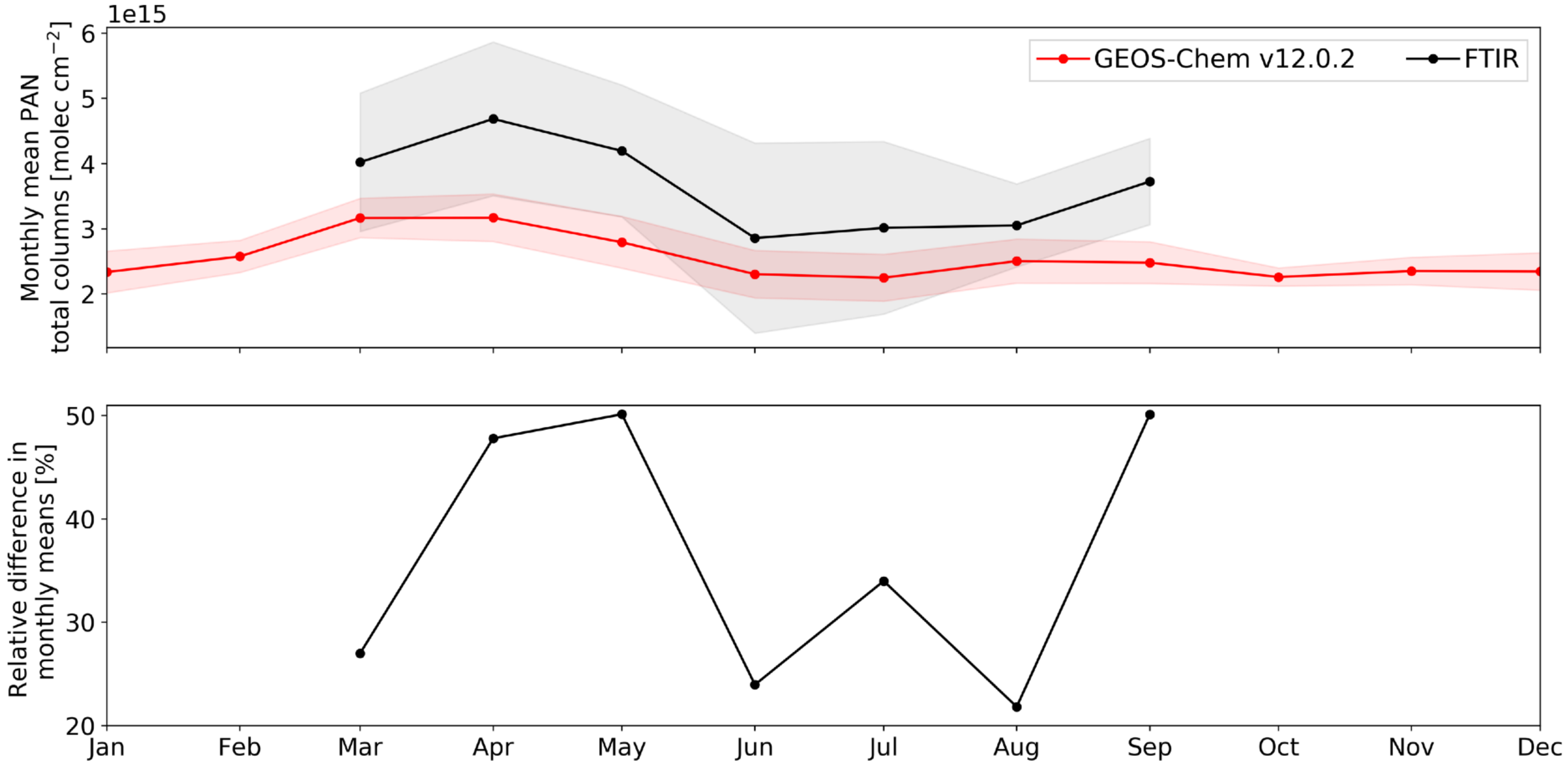

- GEOS-Chem and FTIR capture a similar seasonal cycle
- FTIR observes a higher peak in PAN during the spring months
- Agreement is much closer during the summer months

Results - August 2017 Enhancements

- Two independent, large-scale wildfires occurred in BC and NWT during August 2017
    - The BC fires were record-setting in magnitude, and affected over 1.2×10^6 ha [BC Wildfire Service, 2017]
- The fire plumes were transported to the Arctic and led to the largest measured enhancement in ammonia (NH_3), and enhancements in other tracer species [Lutsch *et al*., 2019]
- Fires are a significant natural source of PAN, we expect to measure an enhancement here

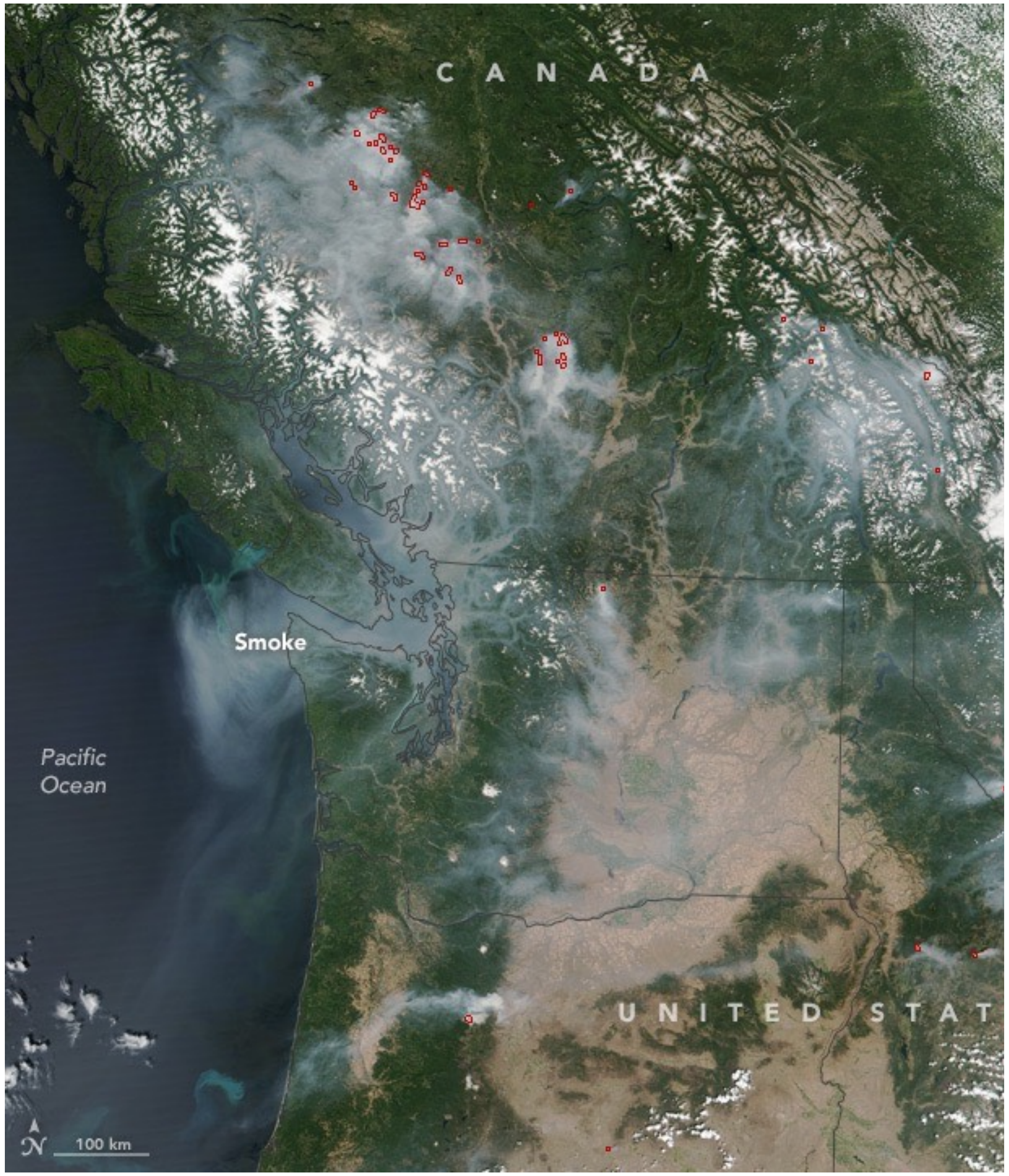

Image credit J. Schmaltz/NASA.

Results - August 2017 Enhancements

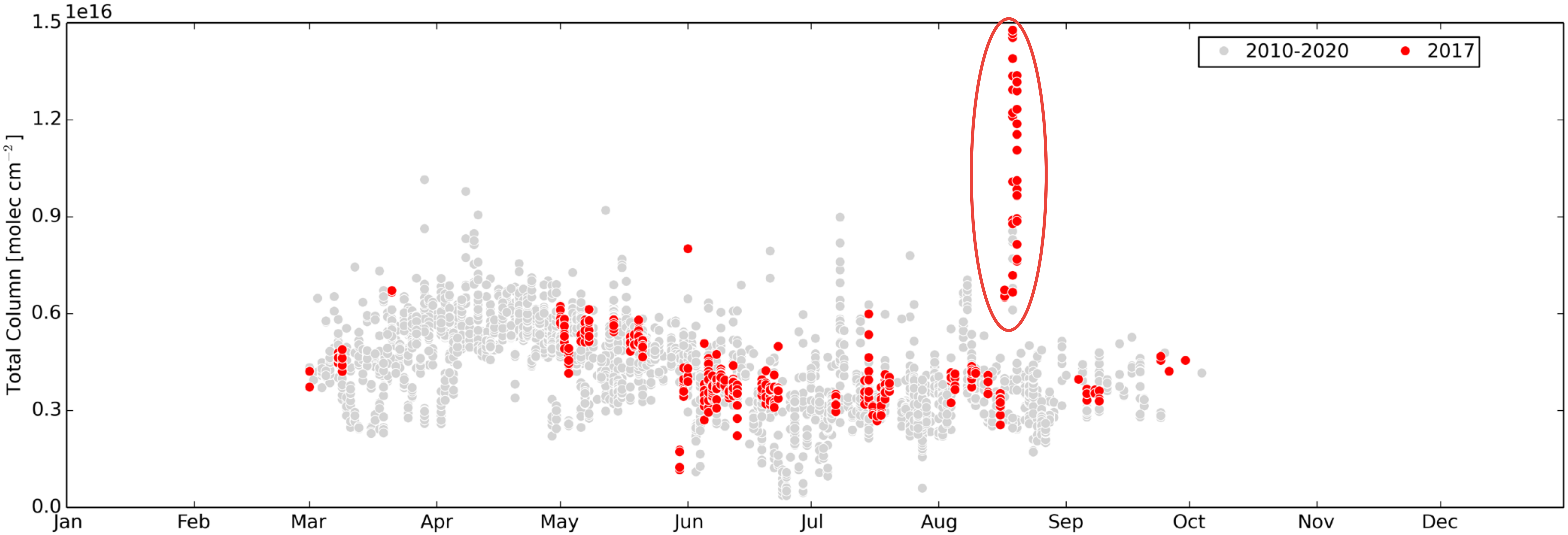

The 2010-2020 time series of PAN total columns with measurements from 2017 highlighted in red, while all other years are plotted in light grey. A large enhancement can be seen in late August, 2017 due to the BC and NWT wildfires.

Results - August 2017 Enhancements

- **Simultaneous enhancements in biomass burning tracer species strongly suggest the observed enhancement in PAN is due to the BC and NWT wildfires**

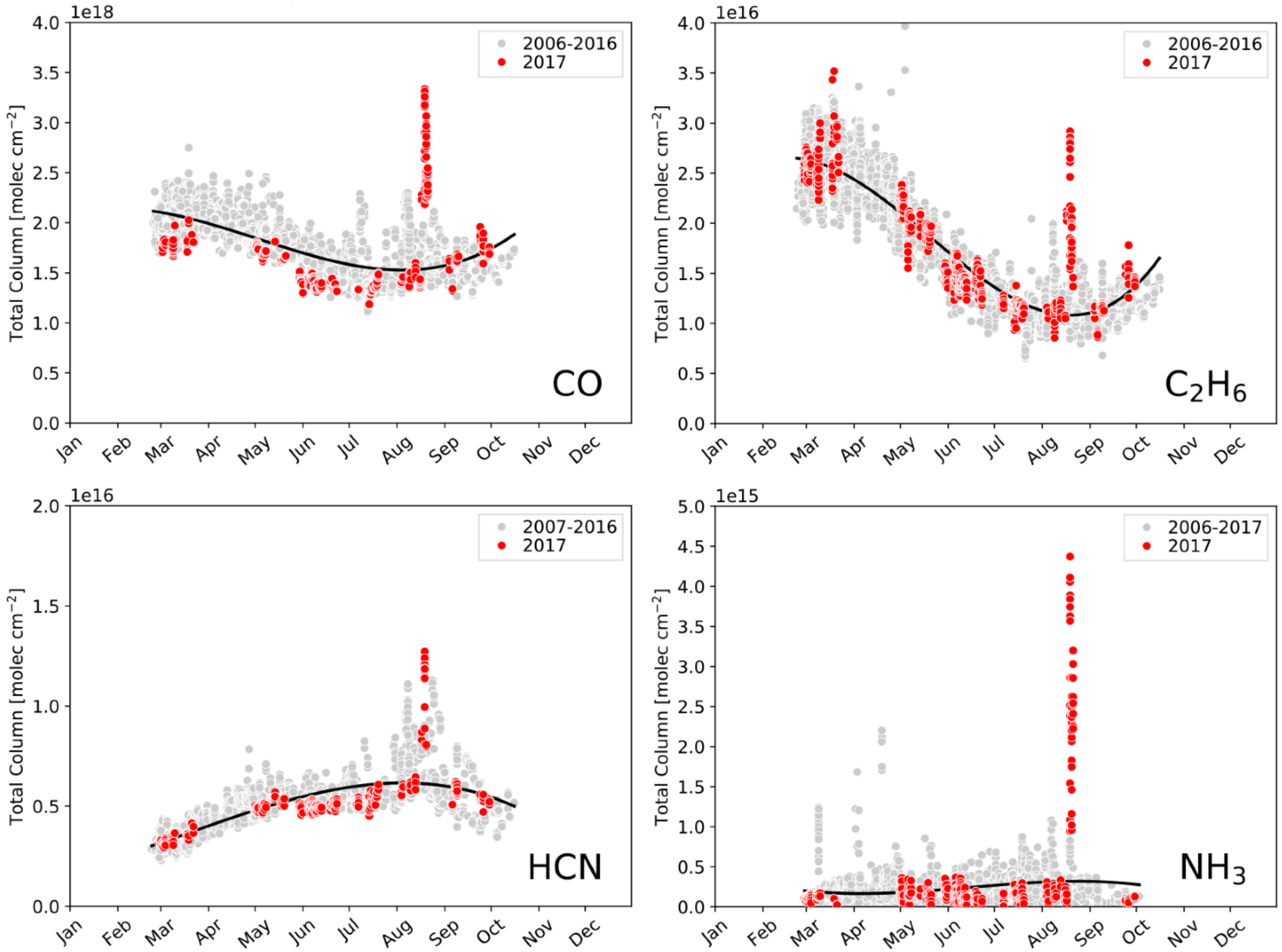

Similar plots to the previous slide, but for CO, HCN, C_2H_6 and NH_3. The black lines denote the mean annual trend. Figure adapted from Lutsch *et al.*, [2019]

Results - August 2017 Enhancements

- To validate our retrievals here, we use measurements from the Infrared Atmospheric Sounding Interferometer (IASI) instruments aboard the MetOp-A & MetOp-B satellites
- Recently, an Artificial Neural Network for IASI (ANNI) retrieval of PAN has been developed [Franco *et al*., 2018]
    - PAN product not yet publicly available, still a WIP
- Strong enhancements during the fire-affected period provided sufficient sensitivity over the plume to retrieve PAN

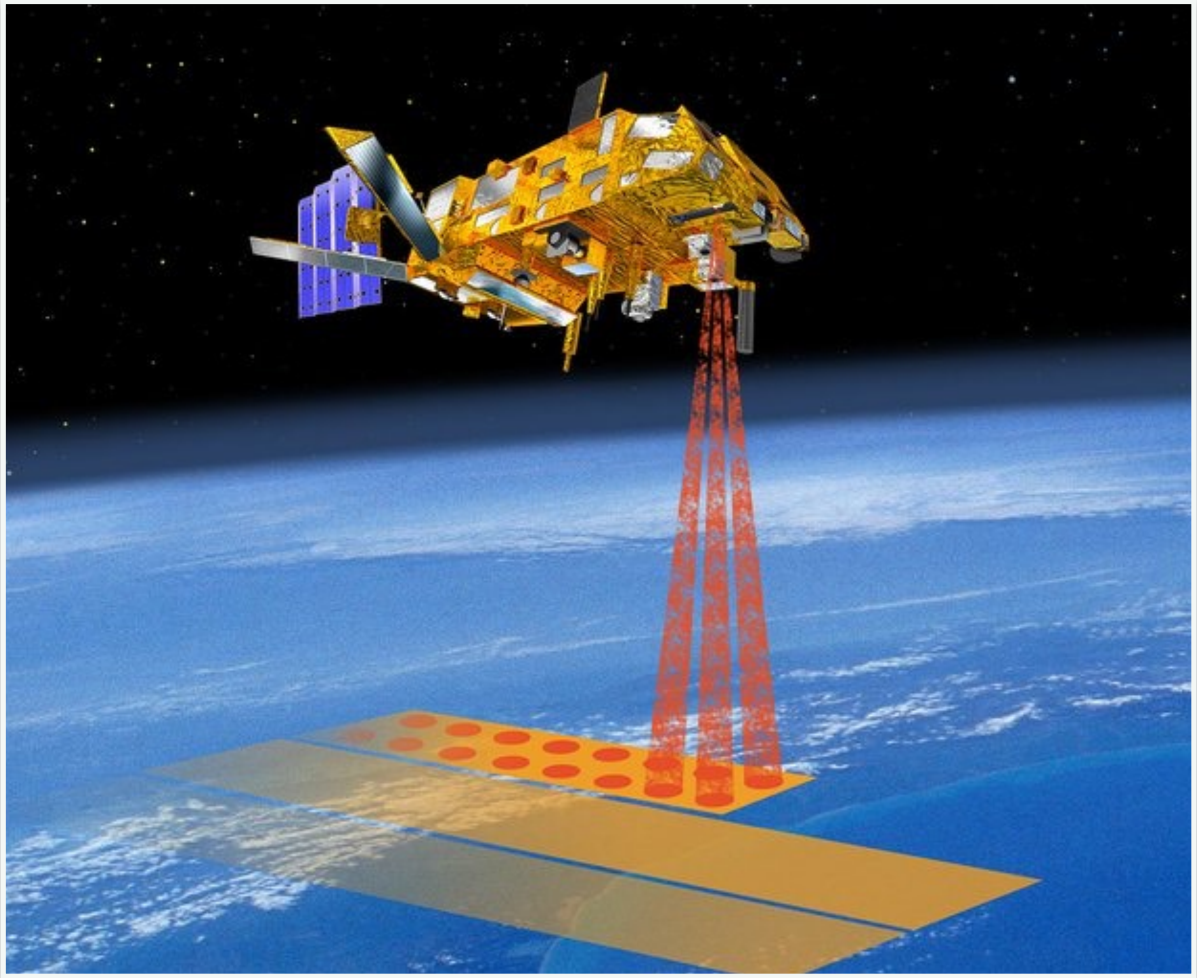

The IASI instrument aboard the MetOP satellite platform. Image credits: EUMETSAT/CNES.

Results - August 2017 Enhancements

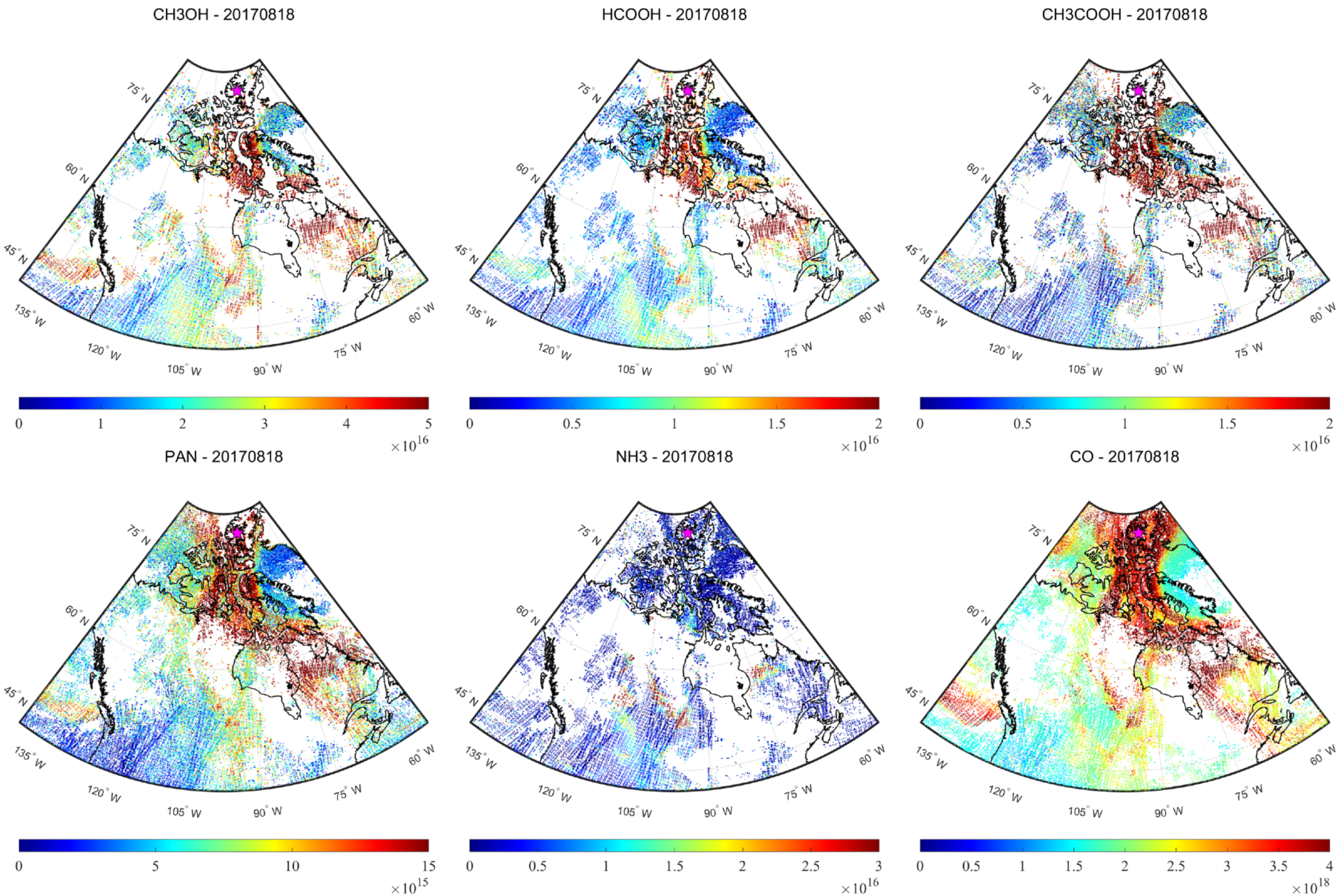

Measurements by IASI-A & B of methanol, formic acid, acetic acid, PAN, ammonia, and carbon monoxide on August 18, 2017. The location of PEARL is denoted by a small purple star. This figure was provided by Bruno Franco from the Université libre de Bruxelles

Results - August 2017 Enhancements

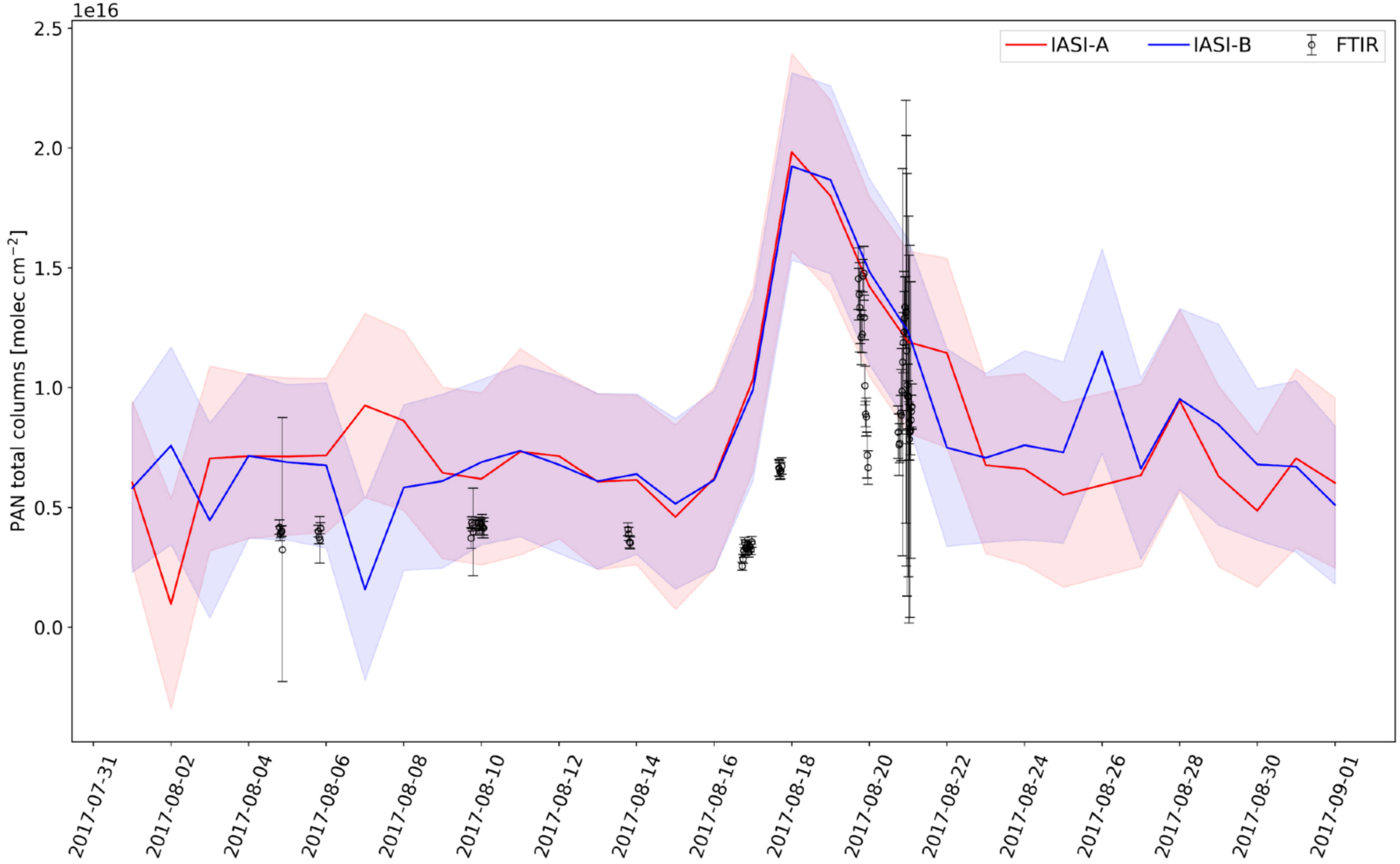

- Computing IASI daily means with 150km of PEARL allows us to more effectively compare measurements
- Good agreement is observed between IASI and the PEARL FTIR during peak enhancement, most measurements fall within the combined bounds of error

Conclusions

- An SFIT4 retrieval scheme has been developed and applied, allowing the retrieval of PAN total columns at PEARL
    - Retrieval performed for 2010-2020; displays a maxima in spring and minima during the summer
- Comparisons with GEOS-Chem v12.0.2 show similar seasonal cycles
    - FTIR observes higher total columns during the spring months, smaller differences during the summer
- Large enhancement in PAN in August 2017 which can be attributed to BC and NWT wildfires
    - Comparisons to IASI-A & B show good agreement during fire-affected period -> Confirmed that wildfires are a source of PAN to the high Arctic

References

Alvarado, M. J., Logan, J. A., Mao, J., Apel, E., Riemer, D., Blake, D., . . . Sager, P. L. (2010). Nitrogen oxides and PAN in plumes from boreal fires during ARCTAS-B and their impact on ozone: An integrated analysis of aircraft and satellite observations. Atmospheric Chemistry and Physics, 10(20), 9739-9760. doi:10.5194/acp-10-9739-2010

Arnold, S., Law, K., Brock, C., Thomas, J., Starkweather, S., Salzen, K. V., . . . Bozem, H. (2016). Arctic air pollution: Challenges and opportunities for the next decade. Elementa: Science of the Anthropocene, 4, 000104. doi:10.12952/journal.elementa.000104

BC Wildfire Service (2017). Wildfire season summary—Province of British Columbia. https://www2.gov.bc.ca/gov/content/safety/wildfire-status/about-bcws/wildfire-history/wildfire-season-summary, Accessed: 2019-7-29

Bey, I., Jacob, D. J., Yantosca, R. M., Logan, J. A., Field, B. D., Fiore, A. M., . . . Schultz, M. G. (2001). Global modeling of tropospheric chemistry with assimilated meteorology: Model description and evaluation. Journal of Geophysical Research: Atmospheres, 106(D19), 23073-23095. doi:10.1029/2001jd000807

Fischer, E. V., Jacob, D. J., Yantosca, R. M., Sulprizio, M. P., Millet, D. B., Mao, J., . . . Deolal, S. P. (2014). Atmospheric peroxyacetyl nitrate (PAN): A global budget and source attribution. Atmospheric Chemistry and Physics, 14(5), 2679-2698. doi:10.5194/acp-14-2679-2014

Fischer, E. V., Zhu, L., Payne, V. H., Worden, J. R., Jiang, Z., Kulawik, S. S., … Flocke, F. (2018). Using TES retrievals to investigate PAN in North American biomass burning plumes. Atmospheric Chemistry and Physics, 18(8), 5639–5653. doi: 10.5194/acp-18-5639-2018

Franco, B., Clarisse, L., Stavrakou, T., Müller, J., Van Damme, M., Whitburn, S., . . . Coheur, P. (2018). A General Framework for Global Retrievals of Trace Gases From IASI: Application to Methanol, Formic Acid, and PAN. Journal of Geophysical Research: Atmospheres, 123(24). doi:10.1029/2018jd029633

Gelaro, R., Mccarty, W., Suárez, M. J., Todling, R., Molod, A., Takacs, L., . . . Zhao, B. (2017). The Modern-Era Retrospective Analysis for Research and Applications, Version 2 (MERRA-2). Journal of Climate, 30(14), 5419-5454. doi:10.1175/jcli-d-16-0758.1

Glatthor, N., Clarmann, T. V., Fischer, H., Funke, B., Grabowski, U., Höpfner, M., . . . Stiller, G. P. (2007). Global peroxyacetyl nitrate (PAN) retrieval in the upper troposphere from limb emission spectra of the Michelson Interferometer for Passive Atmospheric Sounding (MIPAS). Atmospheric Chemistry and Physics, 7(11), 2775-2787. doi:10.5194/acp-7-2775-2007

References

Guenther, A., Karl, T., Harley, P., Wiedinmyer, C., Palmer, P. I., & Geron, C. (2006). Estimates of global terrestrial isoprene emissions using MEGAN (Model of Emissions of Gases and Aerosols from Nature). Atmospheric Chemistry and Physics, 6(11), 3181–3210. doi: 10.5194/acp-6-3181-2006

Law, K. S., & Stohl, A. (2007). Arctic Air Pollution: Origins and Impacts. Science, 315(5818), 1537-1540. doi:10.1126/science.1137695

Law, K. S., Stohl, A., Quinn, P. K., Brock, C. A., Burkhart, J. F., Paris, J., . . . Thomas, J. L. (2014). Arctic Air Pollution: New Insights from POLARCAT-IPY. Bulletin of the American Meteorological Society, 95(12), 1873-1895. doi:10.1175/bams-d-13-00017.1

Liang, Q., Rodriguez, J. M., Douglass, A. R., Crawford, J. H., Olson, J. R., Apel, E., . . . Wisthaler, A. (2011). Reactive nitrogen, ozone and ozone production in the Arctic troposphere and the impact of stratosphere-troposphere exchange. Atmospheric Chemistry and Physics, 11(24), 13181-13199. doi:10.5194/acp-11-13181-2011

Lutsch, E., Strong, K., Jones, D. B., Ortega, I., Hannigan, J. W., Dammers, E., . . . Fisher, J. A. (2019). Unprecedented Atmospheric Ammonia Concentrations Detected in the High Arctic From the 2017 Canadian Wildfires. Journal of Geophysical Research: Atmospheres. doi:10.1029/2019jd030419

Marsh, D. R., Mills, M. J., Kinnison, D. E., Lamarque, J., Calvo, N., & Polvani, L. M. (2013). Climate Change from 1850 to 2005 Simulated in CESM1(WACCM). Journal of Climate, 26(19), 7372-7391. doi:10.1175/jcli-d-12-00558.1

Nordenskiöld, A. E. (1883). Nordenskiöld on the Inland Ice of Greenland. Science, Ns-2(44), 732-738. doi:10.1126/science.ns-2.44.732

Olivier, J.G.J. and J.J.M. Berdowski (2001) Global emissions sources and sinks. In: Berdowski, J., Guicherit, R. and B.J. Heij (eds.) "The Climate System", pp. 33-78. A.A. Balkema Publishers/Swets & Zeitlinger Publishers, Lisse, The Netherlands. ISBN 90 5809 255 0

Ritter, C., Notholt, J., Fischer, J., & Rathke, C. (2005). Direct thermal radiative forcing of tropospheric aerosol in the Arctic measured by ground based infrared spectrometry. Geophysical Research Letters, 32(23). doi:10.1029/2005gl024331

Roiger, A., Schlager, H., Schäfler, A., Huntrieser, H., Scheibe, M., Aufmhoff, H., . . . Arnold, F. (2011). In-situ observation of Asian pollution transported into the Arctic lowermost stratosphere. Atmospheric Chemistry and Physics, 11(21), 10975-10994. doi:10.5194/acp-11-10975-2011

Roiger, A., Thomas, J., Schlager, H., Law, K. S., Kim, J., Schäfler, A., . . . Flemming, J. (2015). Quantifying Emerging Local Anthropogenic Emissions in the Arctic Region: The ACCESS Aircraft Campaign Experiment. Bulletin of the American Meteorological Society, 96(3), 441-460. doi:10.1175/bams-d-13-00169.1

References

Rothman, L., Gordon, I., Barbe, A., Benner, D., Bernath, P., Birk, M., . . . Auwera, J. V. (2009). The HITRAN 2008 molecular spectroscopic database. Journal of Quantitative Spectroscopy and Radiative Transfer, 110(9-10), 533-572. doi:10.1016/j.jqsrt.2009.02.013

Schmale, J., Arnold, S. R., Law, K. S., Thorp, T., Anenberg, S., Simpson, W. R., . . . Pratt, K. A. (2018). Local Arctic Air Pollution: A Neglected but Serious Problem. Earth's Future, 6(10), 1385-1412. doi:10.1029/2018ef000952

Schultz, M.G., Backman, L., Balkanski, Y., Bjoerndalsaeter, S., Brand, R., Burrows, . . . Wittrock, F. (2007). REanalysis of the TROpospheric chemical composition over the past 40 years.

Singh, H. B., Herlth, D., Ohara, D., Zahnle, K., Bradshaw, J. D., Sandholm, S. T., . . . Kanakidou, M. (1992). Relationship of peroxyacetyl nitrate to active and total odd nitrogen at northern high latitudes: Influence of reservoir species on NOx and O3. Journal of Geophysical Research: Atmospheres, 97(D15), 16523. doi:10.1029/91jd00890

Tereszchuk, K. A., Moore, D. P., Harrison, J. J., Boone, C. D., Park, M., Remedios, J. J., . . . Bernath, P. F. (2013). Observations of peroxyacetyl nitrate (PAN) in the upper troposphere by the Atmospheric Chemistry Experiment-Fourier Transform Spectrometer (ACE-FTS). Atmospheric Chemistry and Physics, 13(11), 5601-5613. doi:10.5194/acp-13-5601-2013

van der Werf, G. R., Randerson, J. T., Giglio, L., Collatz, G. J., Mu, M., Kasibhatla, P. S., … Leeuwen, T. T. V. (2010). Global fire emissions and the contribution of deforestation, savanna, forest, agricultural, and peat fires (1997–2009). Atmospheric Chemistry and Physics, 10(23), 11707–11735. doi: 10.5194/acp-10-11707-2010

Viatte, C., Strong, K., Paton-Walsh, C., Mendonca, J., Oneill, N. T., & Drummond, J. R. (2013). Measurements of CO, HCN, and C2H6 Total Columns in Smoke Plumes Transported from the 2010 Russian Boreal Forest Fires to the Canadian High Arctic. Atmosphere-Ocean, 51(5), 522-531. doi:10.1080/07055900.2013.823373

Viatte, C., Strong, K., Walker, K. A., & Drummond, J. R. (2014). Five years of CO, HCN, C2H6, C2H2, CH3OH, HCOOH and H2CO total columns measured in the Canadian high Arctic. Atmospheric Measurement Techniques, 7(6), 1547-1570. doi:10.5194/amt-7-1547-2014

Questions?